Structure-dependent exchange in the organic magnets Cu(II)Pc and Mn(II)Pc

Wei Wu,* A. Kerridge,† A. H. Harker, and A. J. Fisher‡
UCL Department of Physics and Astronomy and London Centre for Nanotechnology, University College London, Gower Street, London WC1E 6BT, United Kingdom

(Received 19 December 2007; revised manuscript received 13 March 2008; published 2 May 2008)

We study exchange couplings in the organic magnets copper(II) phthalocyanine [Cu(II)Pc] and manganese(II) phthalocyanine [Mn(II)Pc] by a combination of Green's function perturbation theory and *ab initio* density-functional theory (DFT). Based on the indirect exchange model, our perturbation-theory calculation of Cu(II)Pc qualitatively agrees with the experimental observations. DFT calculations performed on Cu(II)Pc dimer show a very good quantitative agreement with exchange couplings that our theoretical group extracts by using a global fitting for the magnetization measurements to a spin-$\frac{1}{2}$ Bonner-Fisher model. These two methods give us remarkably consistent trends for the exchange couplings in Cu(II)Pc when changing the stacking angles. The situation is more complex for Mn(II)Pc owing to the competition between superexchange and indirect exchange.

DOI: 10.1103/PhysRevB.77.184403 PACS number(s): 71.10.−w, 71.15.Mb, 71.35.Gg, 71.70.Gm

I. INTRODUCTION

Recently, molecular spintronics[1–5] has become a very active interdisciplinary topic. This is because localized spins in molecular complexes can have very long spin relaxation times (up to of order 1 s),[5] while the chemical engineering of such complexes is much more flexible than is the case in conventional inorganic-semiconductor electronics. The main building blocks of molecular spintronics, namely, radicals containing localized electrons, are promising candidates both for spintronics and for quantum information processing. Against this background, experimental and theoretical studies of the magnetism in spintronics-related organic materials are crucial for the development of devices such as molecular magnetic random-access memory.[6–8]

There is a long history of research on metal phthalocyanines (MPc), because of their commercial applications and excellent electro-optical properties.[9] In particular, their magnetic properties have been extensively studied.[10–12] Mn(II)Pc was one of the first molecular magnets;[13] its properties were shown to depend critically on the stacking of the planar molecular π systems. We define a stacking angle as shown in Fig. 1; the β-Mn(II)Pc crystal (stacking angle of 45°) was found to be ferromagnetic, while the α-Mn(II)Pc thin film (stacking angle of 65°) was shown to be antiferromagnetic. However, there is still debate about the details of the molecular stacking in the α-phase Cu(II)Pc material: transmission-electron diffraction (TED) observations for Cu(II)Pc on a KCl (001) surface[14] suggested that the stacking orientation in the α phase was the so-called × model as shown in Fig. 2(a). However, the most recent TED experiments[15] by contrast indicated that the orientation is the "+" model shown in Fig. 2(b). The arrows in Fig. 2 show the direction of the displacement of the Pc molecules between successive layers; these directions differ by a rotation of 45°. Since this issue is not yet resolved, and given that the substrate used in Refs. 14 and 15 differs from that used in Ref. 16 in the following discussion, we adopt the + model.

Recently Heutz[16] *et al.* have performed further magnetic measurements on different phases of Cu(II)Pc and Mn(II)Pc by using superconducting quantum interference device (SQUID) magnetometry. In the remainder of this paper, we describe these spin systems by using a Heisenberg spin-chain model,[17] which is believed to be a good description for organic systems containing localized spin centers:

$$\hat{H}_{\text{eff}} = -2J \sum \mathbf{S}_i \cdot \mathbf{S}_j. \tag{1}$$

Note that with the sign convention we adopt, a positive exchange constant J corresponds to ferromagnetic coupling, while a negative J describes antiferromagnetic interactions. In these experiments, Mn(II)Pc powder samples (β phase) show strongly ferromagnetic coupling with $J \approx 11.45$ K, while Mn(II)Pc films (α phase) grown on an inert Kapton substrate shows a relatively much weaker antiferromagnetic coupling with $J \approx -1.61$ K. Cu(II)Pc powder (β phase) is found to be very weakly ferromagnetic (indeed nearly paramagnetic) with $J \approx 0$ K, but Cu(II)Pc films (α phase) and Cu(II)Pc whose growth is templated by a layer of 3,4,9,10-perylenetetracarboxylic dianhydride predeposited on the

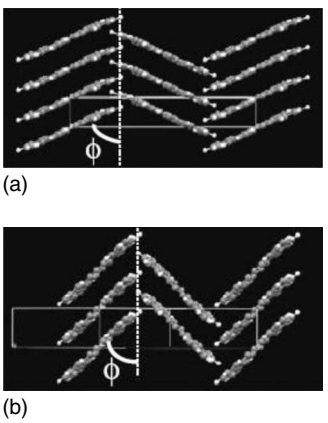

FIG. 1. Schematic arrangements of (a) the α- and (b) β-phase MPc structures. The stacking angle is ϕ in each case.

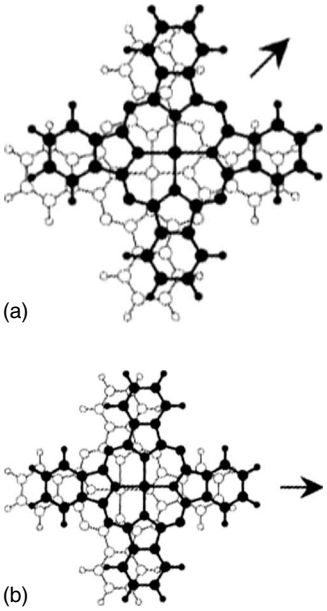

FIG. 2. Two models for stacking orientations for α-Cu(II)Pc: (a) $\times$; (b) $+$.

Kapton substrate are found to be more strongly antiferromagnetic ($J \approx -1.50$ K). The exchange constants for Mn(II)Pc are extracted from the intercept of the inverse susceptibility versus temperature, while those for Cu(II)Pc are found by a global fit of the experimental data to a finite $S=1/2$ Heisenberg spin-chain model (the so-called Bonner-Fisher model[18]). This model is expected to be sufficiently accurate, despite its neglect of interchain couplings, provided the temperature is not too low relative to the exchange constants.

These experiments clearly show the switching of magnitudes and signs of the exchange couplings as the molecular packing varies from phase to phase, and also that the magnetic properties are determined by the structure (α versus β), not by the sample morphology (powder versus thin film). The results confirm the previously measured[10,11] difference between the α and β phases of Mn(II)Pc, and also show that a corresponding difference exists for Cu(II)Pc, although in this case the β phase is paramagnetic rather than ferromagnetic.

Despite the long history of experimental work on MPc, there have been very few systematic theoretical studies of the mechanisms underlying the variation in the exchange interactions; the problem is complicated by the molecular structure and rather weak spin-spin interactions compared to conventional inorganic semiconductors. In this paper, we aim to gain both a picture of the physics driving the structure-dependent exchange and a quantitative understanding of its magnitude, in Cu(II)Pc and Mn(II)Pc.

Our remaining discussion falls into five sections. In Sec. II, we introduce the different mechanisms for exchange and describe state-of-the art quantitative methods to evaluate exchange interactions by using density-functional theory (DFT) and the broken-symmetry concept. We also describe the atomic and electronic structure of the systems we consider. In Sec. III, we perform Green's-function perturbation-theory calculations for exchange interactions to get a rough picture of essential physics. In Sec. IV, we use DFT with the hybrid exchange-correlation functional B3LYP to evaluate the exchange interactions quantitatively. At the end, we draw our conclusions in Sec. V.

II. THEORETICAL OVERVIEW

A. Qualitative description of exchange interactions between localized electrons

The various processes contributing to the exchange interactions between localized spins were extensively considered by Anderson.[19] His original paper considered exchange interactions between magnetic ions in ionic crystals, but the same concepts and arguments apply in the case of the biradical studied here. The *direct* exchange interaction originates from a quantum exchange term of the Coulomb interaction between localized electrons, e.g., *d* electrons in a magnetic ion; this always gives rise to ferromagnetic exchange interactions. However, for MPc, the direct exchange interaction can generally be neglected owing to the large molecular size and the localization of the metal electrons.

The *superexchange* arises from the terms in the Hamiltonian that tend to delocalize electrons. It is then necessary to take the hopping perturbation to higher order in order to reach an excited state in which an electron is transferred onto a neighboring magnetic site. For example, in a simple Hubbard model, the second order in perturbation theory leads to an exchange interaction $-2t^2/U$, where t is the transfer integral between sites and U is the on-site Coulomb repulsion. In a more realistic model, there are many more superexchange pathways but the same principles remain: According to the definition we adopt, for a process to be classified as superexchange, it should proceed through virtual states involving the migration of charge between the magnetic centers. The superexchange mechanism is especially important when the magnetic atoms are separated by nonmagnetic species, for example, inorganic anions or organic ligands, through which charge can pass from one magnetic atom to another. We should note that the superexchange vanishes not only when the distances are large but also when the transfer of electrons between the magnetic centers and these covalent "bridges" is symmetry forbidden.

The indirect exchange interaction between electronic spins is similar to the indirect exchange interaction between nuclear moments, which is mediated by the conduction (or valence) electrons: A polarization of the conduction electrons around one local moment is propagated to another, giving rise to an effective interaction. This nuclear interaction was first discovered by Ruderman and Kittel[21] and independently in molecular physics by Ramsey *et al.*[22,23] and by Bloembergen and Rowland;[24] the generalization to localized electronic moments is due to Kasuya[25] and Yosida.[26] In metals, it leads to a long-range exchange coupling that is oscillatory in sign.

We can sharpen the distinction between the different types of exchange by writing the full electronic Hamiltonian as

$$\hat{H} = \hat{H}_{\text{spin}} + \hat{H}_{\text{ligand}} + \hat{V}_{\text{direct}} + \hat{V}_{\text{hop}} + \hat{V}_{\text{polarize}}. \qquad (2)$$

The terms are defined as follows. $\hat{H}_{\text{spin}}$ corresponds to the isolated spins and $\hat{H}_{\text{ligand}}$ to the rest of the material (decoupled from the spins), both being taken to include an appropriate (spin-independent) mean field. We take $\hat{H}_0=\hat{H}_{\text{spin}}+\hat{H}_{\text{ligand}}$ to be our unperturbed Hamiltonian. $\hat{V}_{\text{direct}}$ then involves the direct Coulomb interaction, coupling the spins to one another without involving the ligands; $\hat{V}_{\text{hop}}$ involves all processes that transfer an electron between the magnetic species and the ligands, while $\hat{V}_{\text{polarize}}$ includes all other (noncharge-transferring) interactions between the magnetic species and the ligands.

We can then develop a perturbation expansion for the full Green's function G (as, for example, in Ref. 20) as

$$G = G_0 + G_0VG_0 + G_0VG_0VG_0 + \cdots , \tag{3}$$

where V is the perturbation $\hat{V}_{\text{direct}}+\hat{V}_{\text{hop}}+\hat{V}_{\text{polarize}}$ and G_0 is the Green's function corresponding to unperturbed Hamiltonian. The effective exchange is then recovered by computing an effective Hamiltonian

$$E - \hat{H}_{\text{eff}} = G^{-1} \tag{4}$$

within a ground-state manifold of configurations differing only in the spin orientations. Within this picture, the direct exchange corresponds to the first-order term involving $\hat{V}_{\text{direct}}$, while superexchange and indirect exchange correspond to higher-order terms involving $\hat{V}_{\text{hop}}$ and $\hat{V}_{\text{polarize}}$, respectively. It is clear from the definitions of the various terms in $\hat{V}$ that the virtual states that couple to the ground-state manifold are orthogonal; therefore (at least to low orders in $\hat{V}$), we do not need to consider cross-terms between the different operators.

In this paper, we will neglect $\hat{V}_{\text{direct}}$, for the reasons given above. Appropriate expressions for $\hat{V}_{\text{hop}}$ and $\hat{V}_{\text{polarize}}$ are given in Sec. III below.

B. Quantitative calculation: Density-functional theory calculations of exchange couplings in biradicals

DFT[27–33] is a powerful tool for accurate prediction of the exchange interactions in chemically complex wide-gap materials. However, current density functionals, based on Kohn-Sham theory, give a poor representation of singlet states containing a pair of localized electron spins since the Kohn-Sham orbitals are constrained to respect the symmetry of the system and are therefore generally formed from linear combinations of the single-center wave functions. One has to use instead a so-called broken-symmetry method,[29] in which the magnetic orbitals are localized in different radical centers, with their spins oppositely aligned. Recently, Martin and Illas[32,33] checked the performance of different exchange-correlation functionals in the calculation of magnetic couplings and found that the choice of exchange functionals is extremely important, while the role of the correlation functional is minor. Although the precise reasons are unclear, it is empirically found that it is necessary to mix some proportion of exact exchange into the functional in order to obtain results that agree with experiment or with higher-quality quantum chemistry results for small molecules; crudely, this may be understood as requiring some balance between the overlocalization of electrons in a Hartree-Fock calculation and the excessive delocalization in standard density functionals. In particular, the B3LYP functional,[35–37] which mixes about one-quarter Hartree-Fock exchange, has been found to give good results for dinuclear molecules, organic biradicals, and spins localized at defects in carbon-containing materials.[32–34] In Sec. IV, we perform DFT with B3LYP exchange-correlation functional to calculate exchange interactions in Cu(II)Pc dimers based on this broken-symmetry concept.

Although the DFT and perturbative approaches to the problem appear at first sight to be quite different, one can think of them as representing in different ways the same response of the electronic system to its spin-dependent interactions. In the case of the DFT, this response is represented as a change in the Kohn-Sham states, while in the model approaches, the many-electron wave function responds by including small admixtures of excited-state configurations.

C. Electronic structure of isolated Cu(II)Pc and Mn(II)Pc

Before we perform the perturbation-theory calculation for the exchange interaction, we need to understand the nature of the one-electron states in the isolated molecules. We used the GAUSSIAN 98 code,[38] performing a DFT calculation with the B3LYP[37] exchange-correlation functional and a 6-31G (Ref. 39) basis set to optimize the molecular geometry of isolated Cu(II)Pc and Mn(II)Pc molecules. We then use the key Kohn-Sham states emerging from DFT calculation which are nearest to the highest occupied molecular orbital-lowest unoccupied molecular orbital (LUMO) gap as a basis to perform a separate perturbation-theory calculation.

Our level scheme for Cu(II)Pc is shown in Fig. 3(a). The states are labeled by the irreducible representations of the D_{4h} point group. From the Mulliken population analysis, we can identify b_{1g} as a metal d orbital which is hybridized with the Pc ring (Mulliken charge 0.30). The total Mulliken charge on copper is +0.97. The total Mulliken spin density on the copper atom is 0.68; this is consistent with the existence of one singly occupied orbital, with a spin mainly but not entirely localized on the copper atom. The overall symmetry of the electronic state is $^2B_{1g}$. We found that the occupied molecular orbital with the largest Kohn-Sham eigenvalue is not the singly occupied b_{1g} state, but the a_{1u} state; this is slightly different from the early extended Hückel calculations.[40] This highlights the importance of two-electron Coulomb terms in determining the configuration: doubly occupying the b_{1g} state would incur a large Coulomb penalty because the charges would spend much of their time localized in the Cu $3d$ states, whereas the double-occupancy penalty for the more diffuse a_{1u} state is much smaller.

For Mn(II)Pc, the expected total spin is $S=3/2$.[10,16] Our Gaussian calculation gave the overall electronic configuration $^4A_{1g}$, with three singly occupied one-electron levels having a_{1g} and e_g (twice) symmetries. The total Mulliken charge on Mn is +1.14; again, this is of the same order as, but somewhat less than, the nominal +2 valence. The Mulliken

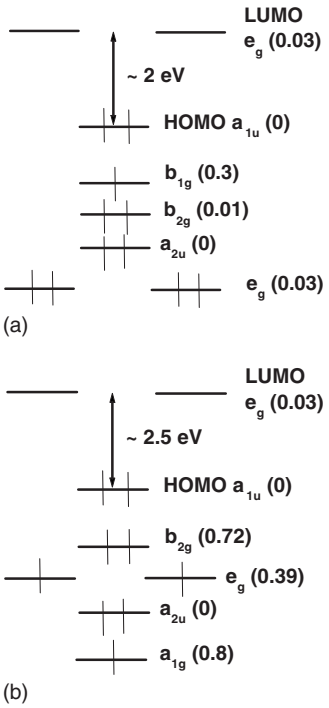

FIG. 3. The schematic of the key states from our Gaussian DFT calculations of the electronic structures of isolated (a) Cu(II)Pc and (b) Mn(II)Pc. The majority-spin contributions to the Mulliken charge on the transition-metal atoms are shown in brackets (the minority-spin contributions for the doubly occupied states are similar).

spin density on the Mn atom is +3.1. Our calculation results are similar to those in Ref. 40 which give ${}^4A_{2g}$ total symmetry and the same single-occupied states. However, this picture of the electronic structure is not the only one. Liao[41] also used DFT methods and found an electronic configuration in which the three unpaired electrons occupy the a_{1g}, b_{2g}, and one e_g state, while the other e_g state is doubly occupied, to give an electronic symmetry ${}^4E_g$. This calculation is in agreement with the more recent magnetic circular dichroism and UV-visible measurements[42] of the molecule in an argon matrix but differs from the early magnetic measurements of solid Mn(II)Pc. It is possible that the ${}^4E_g$ configuration (which would lead to a Jahn-Teller distortion, because of its orbital degeneracy) may be favored in the isolated molecule or in the argon matrix, with the ${}^4A_{2g}$ state favored in the bulk material (where no Jahn-Teller distortion has been observed).

III. GREEN'S FUNCTION PERTURBATION CALCULATIONS

A. Superexchange calculation

We aim to understand the mechanism of exchange couplings between neighboring Mn(II)Pc and Cu(II)Pc molecules observed in experiments.[10,11,16] We first consider the superexchange contributions.

1. Cu(II)Pc

As explained in Sec. II, the superexchange contribution is generally dominant when considering the exchange interaction between localized spins in insulating materials. However, Cu(II)Pc is an example of a situation where this interaction is expected to be negligible. This is because the unpaired spin is located in a b_{1g} orbital,[40] but there is no low-energy state of b_{1g} symmetry in the ligand available to hybridize with it. Therefore, as long as the symmetry of the molecule remains D_{4h} (believed to be an excellent approximation even in the crystal), the spin-carrying electron is "tied" to the Cu site and no superexchange can take place except by direct hopping from the Cu orbitals onto the neighboring molecule. The amplitude for this process is expected to be very small.

2. Mn(II)Pc

In the case of Mn(II)Pc, there are three unpaired electrons per molecule occupying the a_{1g}, e_{gx}, and e_{gy} molecular orbitals (see Sec. II C). We can call these metal states because these orbitals originate from the splitting of atomic $3d$ states in the molecular environment which has D_{4h} symmetry. The two $S=3/2$ spins of the individual molecules can be combined to form a total spin of 0,1,2,3. We therefore need, in principle, three independent parameters in the spin Hamiltonian to characterize fully the relative energies of these states. If we neglect spin-orbit coupling, the Hamiltonian must be invariant under simultaneous rotations of both spins and therefore must have the form

$$\hat{H} = -J_1(\mathbf{S}_A \cdot \mathbf{S}_B) - J_2(\mathbf{S}_A \cdot \mathbf{S}_B)^2 - J_3(\mathbf{S}_A \cdot \mathbf{S}_B)^3, \tag{5}$$

where J_1, J_2, and J_3 are exchange couplings and A, B label the molecules. We can find all three parameters from the 4×4 Hamiltonian matrix spanned by the states with total z spin angular momentum $M_S=0$: $|(3/2)_A,(-3/2)_B\rangle$, $|(1/2)_A,(-1/2)_B\rangle$, $|(-1/2)_A,(1/2)_B\rangle$, and $|(-3/2)_A,(3/2)_B\rangle$. We use a similar method to that described in Ref. 20: We construct the effective Hamiltonian based on an extended Hubbard model by Green's-function perturbation theory, compare this with Eq. (5), and extract the exchange constants. For simplicity, we include only intermediate states where a single electron is transferred between adjacent Mn ions via the ligand e_g states (i.e., we neglect the possibility that two or more electrons transfer together). We also neglect direct electron transfer between the d states of the Mn ions, because these states are quite well localized. Our extended Hubbard model reads

$$\hat{H} = \hat{H}_0 + \hat{H}_t + \hat{H}_p, \tag{6}$$

$$\begin{aligned}\hat{H}_0 = \Bigg\{ & \sum_i E_i \hat{n}_i + v_{pmn}(\hat{n}_{E_{gx}A} + \hat{n}_{E_{gy}A})(\hat{n}_{e_{gx}A} + \hat{n}_{e_{gy}A} + \hat{n}_{a_{1g}A}) \\ & + u_{gx}\hat{n}_{a_{1g}A}(\hat{n}_{e_{gx}A} + \hat{n}_{e_{gy}A}) + u_{xx}(\hat{n}_{e_{gx}A\uparrow}\hat{n}_{e_{gx}A\downarrow} + \hat{n}_{e_{gy}A\uparrow}\hat{n}_{e_{gy}A\downarrow}) \\ & + u_{gg}\hat{n}_{a_{1g}A\uparrow}\hat{n}_{a_{1g}A\downarrow} \Bigg\} + \{A \Leftrightarrow B\},\end{aligned} \tag{7}$$

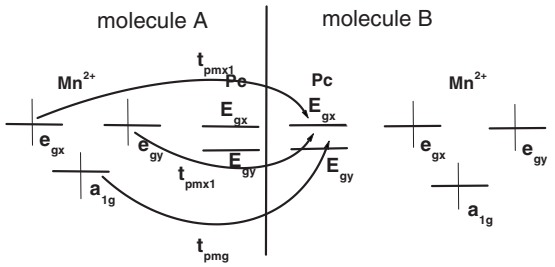

FIG. 4. The possible intermolecular transitions.

$$\hat{H}_t = \Bigg\{ \sum_{\sigma} [t_{pmg}\hat{c}^{\dagger}_{(a_{1g}A)\sigma}(\hat{c}_{(E_{gx}B)\sigma} + \hat{c}_{(E_{gy}B)\sigma}) + t_{pmx1}(\hat{c}^{\dagger}_{(e_{gx}A)\sigma}\hat{c}_{(E_{gx}B)\sigma} + \hat{c}^{\dagger}_{(e_{gy}A)\sigma}\hat{c}_{(E_{gy}B)\sigma}) + t_{pmx2}(\hat{c}^{\dagger}_{(e_{gx}A)\sigma}\hat{c}_{(E_{gy}B)\sigma} + \hat{c}^{\dagger}_{(e_{gy}A)\sigma}\hat{c}_{(E_{gx}B)\sigma}) + \text{H.c.}] \Bigg\} + \{A \Leftrightarrow B\}, \tag{8}$$

$$\hat{H}_p = -K\mathbf{s}\cdot\mathbf{S}. \tag{9}$$

Here, a_{1g}, e_{gx}, and e_{gy} label the metal states; E_{gx} and E_{gy} label LUMO ligand states for distinguishing metal and ligand e_g states.[9] $\hat{H}_0$ includes the single-particle energies E_i, where i runs through a_{1g}, e_{gx}, e_{gy}, E_{gx}, E_{gy}, the Coulomb interaction between metal and ligand states, and the on-site Coulomb interactions. There are two parts in the perturbation: one is $\hat{H}_t$ which transfers electrons between molecules and the other is $\hat{H}_p$ representing the interaction between $\frac{1}{2}$ spin ($\mathbf{s}$) in the ligand and $\frac{3}{2}$ spin ($\mathbf{S}$) on the metal within the molecule. We suppose that $\hat{H}_p$ is itself ultimately a representation of a further superexchange process and therefore, like $\hat{H}_t$, originates in V_{hop} as defined in Sec. II A. t_{pmg}, t_{pmx1}, and t_{pmx2} are the intermolecular hopping integrals shown in Fig. 4, E_g and e_g are the energies of ligand and metal e_g states relative to the energy level of a_{1g} state, u_{gx} is Coulomb interaction between the a_{1g} and e_g levels, u_{xx} is the Coulomb interaction between two degenerate Mn e_g states, and v_{pmn} is the Coulomb interaction between the Mn and Pc states within a molecule.

From this Hamiltonian, we can see when one electron is transferred from the metal state of molecule A to the ring state of molecule B where it can interact with the Mn spin; it is through the interaction $\hat{H}_p$ that the spin projections m_A and m_B associated with the two molecules can change, thereby coupling the four spin states: $|(3/2)_A,(-3/2)_B\rangle$, $|(1/2)_A,(-1/2)_B\rangle$, $|(-1/2)_A,(1/2)_B\rangle$, and $|(-3/2)_A,(3/2)_B\rangle$. Note that in D_{4h} symmetry, the e_g states of Mn can hybridize effectively with the e_g states of the ring; the existence of unpaired spins in the e_g states is what makes superexchange processes much more important in the case of Mn(II)Pc.

There are 25 spatial configurations and each has four possible spin states, giving a total of 100 states. We construct the 100×100 Hamiltonian matrix for $\hat{H}_0$ and V and then extract the effective Hamiltonian within the 4×4 low-energy subspace by using Green's function perturbation theory[20] to calculate the energy shifts. By comparing this low-energy subspace with the $\frac{3}{2}$-spin coupling matrix, we find that it can be written in form (5), with parameters

$$J_1 = \frac{4}{3}K\left[\frac{t^2_{pmg}}{(-E_g+2u_{gx}-3v_{pmn})^2} + \frac{t^2_{pmx1}}{(e_g-E_g+u_{gx}+u_{xx}-3v_{pmn})^2} + \frac{t^2_{pmx2}}{(e_g-E_g+u_{gx}+u_{xx}-3v_{pmn})^2}\right] + O(t^3), \tag{10}$$

$$J_2 = -\frac{4}{9}K^2\left[\frac{t^2_{pmg}}{(-E_g+2u_{gx}-3v_{pmn})^3} + \frac{t^2_{pmx1}}{(e_g-E_g+u_{gx}+u_{xx}-3v_{pmn})^3} + \frac{t^2_{pmx2}}{(e_g-E_g+u_{gx}+u_{xx}-3v_{pmn})^3}\right] + O(t^3), \tag{11}$$

$$J_3 = \frac{4}{27}K^3\left[\frac{t^2_{pmg}}{(-E_g+2u_{gx}-3v_{pmn})^4} + \frac{t^2_{pmx1}}{(e_g-E_g+u_{gx}+u_{xx}-3v_{pmn})^4} + \frac{t^2_{pmx2}}{(e_g-E_g+u_{gx}+u_{xx}-3v_{pmn})^4}\right] + O(t^3). \tag{12}$$

We note several features of this result. First, the dominant terms are those proportional to t^2, i.e., where electrons are exchanged once between the molecules, as expected in a superexchange process. Second, the leading term in J_1 is proportional to Kt^2, in J_2 to K^2t^2, and in J_3 to K^3t^2; this is because $\hat{H}_p$ only couples states in which m_A and m_B alter by one unit of angular momentum. Finally, assuming that the Coulomb energies are all large and positive, J_1 is *always* the same sign as K, irrespective of the values of the various hopping terms. In general, we expect that K, since it is dominated by superexchange, will be negative (corresponding to antiferromagnetic coupling in our sign convention) and therefore J_2 will also lead to antiferromagnetic coupling *independent of the orientation of the molecules*.

Our conclusion about the failure of the superexchange interaction to change sign contrasts sharply with the explanation given by Barraclough *et al.*[10] and by Yamada *et al.*[11] for their experimental results, which they ascribe to the competition between different super-exchange pathways operating via nitrogen atoms. However, this argument fails to take into account correctly the spin algebra—in particular, it ignores the fact that the three electron spins on each Mn atom are, in fact, tied together via strong intra-atomic Coulomb interactions and so cannot be flipped independently.

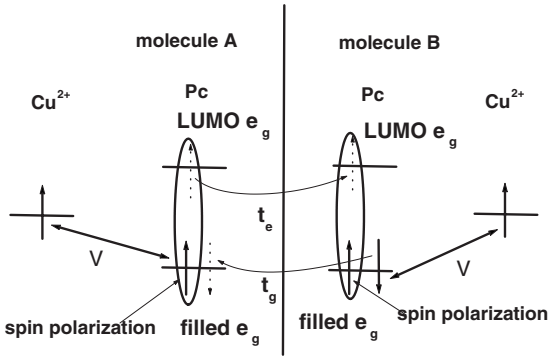

FIG. 5. Cu(II)Pc electron configuration and indirect exchange scheme diagram. This scheme involves two filled e_g states and two empty e_g states (LUMO).

B. Indirect exchange calculation

1. Cu(II)Pc

For the indirect exchange scheme in the Cu(II)Pc dimer (Fig. 5), the unpaired electron spin on the metal polarizes the ligand by the two-body Coulomb interaction; this spin polarization can transfer to the neighboring molecule by orbital hybridization and there interacts with the unpaired spin of the neighboring molecule's metal ion.

Because the LUMOs are e_g ligand states, we should consider the filled ligand states with the same symmetry. The two-body Coulomb interaction can be represented in second-quantized form as

$$\hat{v} = \sum_{\sigma\sigma'} \sum_{ABDE} \left[\int d\mathbf{r} d\mathbf{r}' \psi_A^*(\mathbf{r}) \psi_B^*(\mathbf{r}') \frac{1}{|\mathbf{r}-\mathbf{r}'|} \psi_D(\mathbf{r}') \psi_E(\mathbf{r}) \right] \times \hat{c}_{A,\sigma}^\dagger \hat{c}_{B,\sigma'}^\dagger \hat{c}_{D,\sigma'} \hat{c}_{E,\sigma}, \quad (13)$$

where $\hat{c}$ and $\hat{c}^\dagger$ are the electron annihilation and creation operators, and A,B,D,E may each represent a metal orbital or a ligand orbital. Since we wish to consider processes in which the net charge of the metal ion does not change (i.e., contributions to $\hat{V}_{\text{polarize}}$ rather than $\hat{V}_{\text{hop}}$ in the language of Sec. II A), one of (A,B) should correspond to a Cu state, i.e., metal b_{1g} state and one to a Pc state, e.g., ligand e_g state and similarly for (D,E).

Hence, overall, the four indices may involve one entry for an e_g LUMO state, two entries for the b_{1g} state, and one entry for a doubly filled ligand state: the highest-lying such states are a_{1u}, a_{2u}, or b_{2g} ligand states for single-molecule electronic structure.[9] However, because a_{1u} and a_{2u} are odd under inversion, but b_{1g} and e_g are even, the two-electron integrals involving a_{1u} and a_{2u} are zero. Furthermore, B_{2g} transforms like xy in D_{4h} symmetry, b_{1g} like x^2-y^2, and $e_{gx,y}$ like zx, zy. The two-electron integral involving b_{2g} is therefore odd in either y or in x depending which e_g state appears. So, in fact, the only important doubly occupied states are the filled e_g states which appear slightly below the a_{1u} and a_{2u}.

In order to simplify the calculation, we assume that there is only one electron-hole pair produced in the Cu(II)Pc dimer (additional electron-hole pairs will cost more energy). As in Sec. III A 2, we need consider only the situation where $M_{\text{dimer}}^{\text{total}} = M_{total}^A + M_{total}^B = 0$ in order to extract the exchange constant. We find that the Hamiltonian $\hat{v}$ can be written as the linear combination of the product of the metal spin operators and ligand spin-polarization operators owing to the preservation of total S_z in the isolated molecule. We label the spatial LUMO state of the ligand by using "X," the filled states "G," and metal b_{1g} state "b." We use the following notation for the two-electron integrals:

$$\{a,b|c,d\} = \int d\mathbf{r} d\mathbf{r}' a(\mathbf{r})^* b(\mathbf{r}')^* \frac{1}{|\mathbf{r}-\mathbf{r}'|} c(\mathbf{r}) d(\mathbf{r}'). \quad (14)$$

We can now apply Green's-function perturbation theory[20] to this problem; the perturbation includes the Coulomb interaction $\hat{v}$ which can polarize the spin in a ligand and hopping t that transfers this polarization from one molecule to another. We find that the leading term J_1 in the spin-$\frac{1}{2}$ couplings is given by

$$J_1 = \frac{4\alpha^2 t}{(U_g - U_x - E_x - 2j_{\text{eh}})^2}, \quad (15)$$

$$\alpha = 2\{X,b|b,G\}, \quad (16)$$

$$U_g = \{G,G|G,G\}, \quad (17)$$

$$U_x = \{G,X|G,X\}, \quad (18)$$

$$j_{\text{eh}} = \{G,X|X,G\}. \quad (19)$$

α measures the Cu spin's ability to polarize the ligand, U_g is the Coulomb interaction between electrons in the filled E_g state, U_x is the Coulomb interaction between electron and hole within one molecule, j_{eh} is the electron-hole exchange integral, and E_x is energy gap between LUMO and filled e_g state. From Eq. (15), we can see that the magnitude and sign of J_1 depend on the intermolecule transfer integral t. We calculate the matrix element t for polarization transfer by considering the individual hole and electron hoppings among the four states below (Fig. 6). We find $t = \frac{2t_e t_g}{E_x + U_x}$, where $t_{g,e}$ are the single-particle transfer integrals between the filled states and LUMO of different molecules, respectively.

If we consider the contributions from both components of e_g symmetry, the total transfer integral reads

$$t = \frac{t^x + t^y}{u + E_x}, \quad (20)$$

$$t^x = t_e^x t_g^x, \quad (21)$$

$$t^y = t_e^y t_g^y, \quad (22)$$

$$t_e^i = \langle e_{g,i}^{\text{A,LUMO}} | \hat{H}_{core} | e_{g,i}^{\text{B,LUMO}} \rangle, \quad (23)$$

$$t_g^i = \langle e_{g,i}^{\text{A,filled}} | \hat{H}_{core} | e_{g,i}^{\text{B,filled}} \rangle, \quad (24)$$

where $i \in \{x,y\}$, and $\hat{H}_{core}$ is the core Hamiltonian for a Cu(II)Pc dimer. In the present calculations, we evaluate $\hat{H}_{core}$

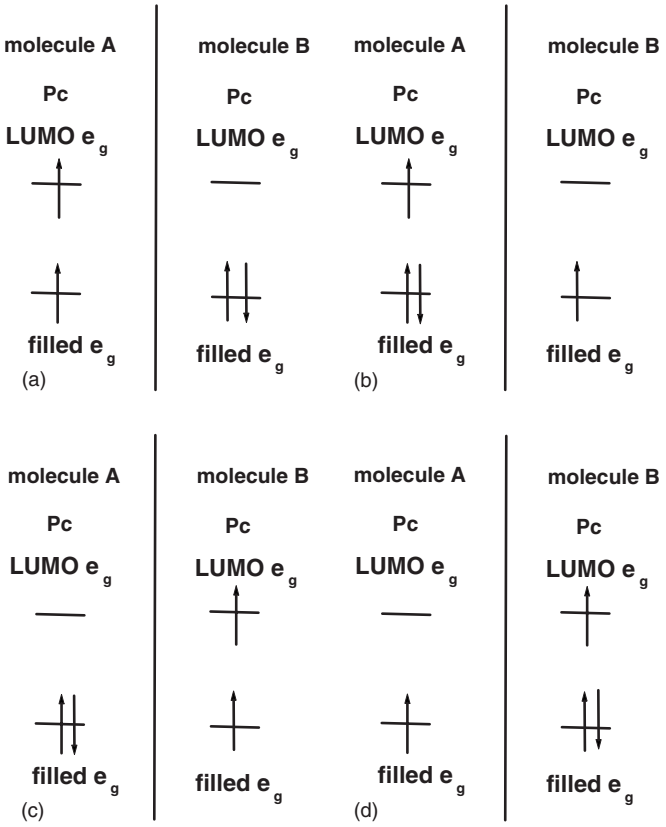

FIG. 6. The four states for calculating the transfer integrals between polarized triplet states of different molecules as the example.

using the GAUSSIAN 98 code,[38] using the same basis set and exchange-correlation functional described above. The symbols A and B refer to these two molecules, and $|e_g^{A,B}\rangle$ refer to the e_g-symmetry single-molecule ligand states belonging to molecule A or B.

We use the single-molecule orbital coefficients of the isolated molecules and the core Hamiltonian for the molecular dimer to calculate the transfer integrals t_e, t_g in the molecular configurations with different stacking angles (20°–90°) as shown in Fig. 1. The distance between these two planes is 3.4 Å.[10,15] In Fig. 7, we show the variation of intermolecule hopping integrals with stacking angle; t_g and t_e change both magnitude and sign with stacking angle. This contributes to corresponding changes in the polarization hopping matrix element t and the exchange constant J_1.

In Fig. 8, we display t^x+t^y, which contributes the dependence on stacking angle to t and hence to J_1, as a function of stacking angle in the range 20°–90°. When the angle is equal to 45°, we find weak ferromagnetic (nearly paramagnetic) coupling. When the angle is equal to 65°, the magnetic interaction is relatively strong antiferromagnetic. This calculation qualitatively agrees with the experimental results,[16] though this calculation cannot predict the absolute magnitude of the exchange coupling.

2. Mn(II)Pc

The Mn(II)Pc calculation is more complicated because there are three unpaired electrons per molecule which occupy

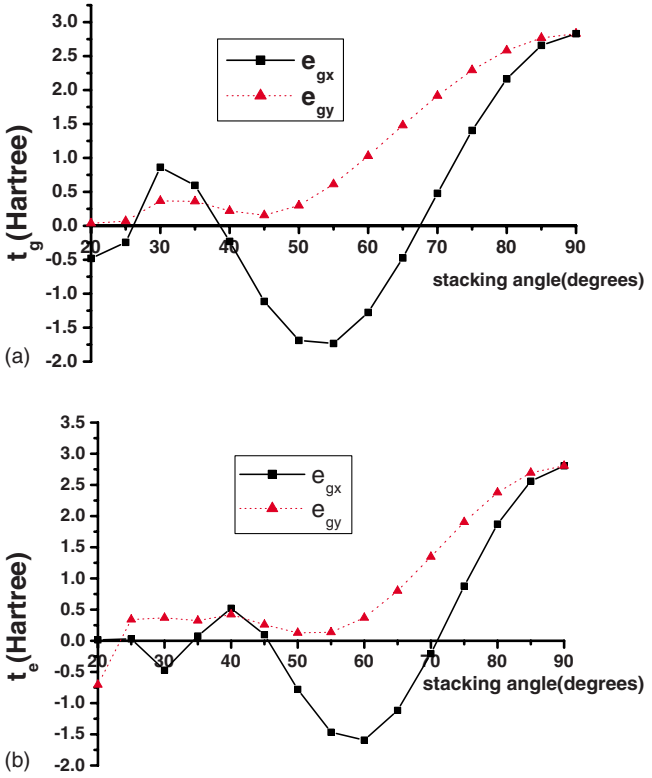

FIG. 7. (Color online) The variation in hopping integrals defined in Eqs. (20)–(24) with stacking angle: (a) t_g for the filled e_g states and (b) t_e for the empty e_g states. In each figure, the solid black curve with square points denotes hopping integrals between x-oriented states of the different molecules, and the dashed red curve with triangular points shows the integrals between y-oriented states.

a_{1g} and e_g states, so it is necessary to use group theory to simplify the calculation of the two-electron integrals. By a similar procedure to Cu(II)Pc (the details are shown in the Appendix), we find a weak ferromagnetic interaction when the stacking angle is 45° but a relatively strong antiferromagnetic interaction for 65°. Unfortunately, even when combined with the superexchange results for Mn(II)Pc obtained in Sec. III A 2 (which always produce antiferromagnetic exchange),

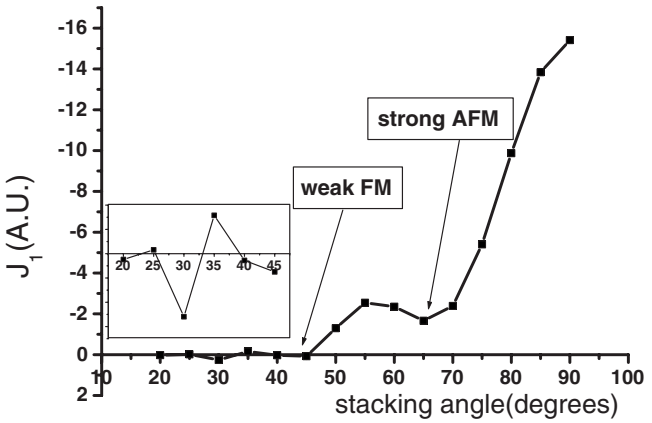

FIG. 8. Variation of the indirect exchange J_1 with the stacking angles shown in Fig. 1; arbitrary units (A.U.) are used.

this result disagrees with the experimental observation of strong ferromagnetic coupling near $\phi=45°$.

IV. *AB INITIO* DENSITY-FUNCTIONAL THEORY CALCULATIONS

Cu(II)Pc

We carry out self-consistent calculations of the electronic structure for molecular dimers for the + structural model at different stacking angles (Fig. 1) by using the Gaussian code with a 6-31G basis set[38] and the unrestricted B3LYP (UB3LYP) exchange-correlation functional.[36,37] We perform calculations for different stacking angles ranging from 20° to 90° as shown in Fig. 10; we have tested the convergence of our results with respect to basis set by performing a calculation with a 6-31+G* basis set (which includes additional polarization functions and diffuse functions) at a single stacking angle (45°) and find negligible changes. We compare directly the DFT total energies and hence calculate the exchange splitting from the difference of the total energies of the broken-symmetry low-spin state and high-spin state. For all stacking angles, we find it necessary to optimize carefully the occupancy of the Kohn-Sham orbitals in order to ensure that there is no charge disproportionation between the molecules; our lowest-energy converged states have Mulliken charges of approximately +1.00, and nominal spin populations of ± 0.68, on each Cu atom. We also need to ensure that the numerical convergence error in the DFT calculations is much smaller than the order of the exchange couplings (1 K $\sim 10^{-6}$ hartree); in our calculations, we converge to at least 10^{-9} hartree. It is encouraging that we find negligible spin contamination in our final Kohn-Sham wave functions, i.e., the $\langle \hat{S}^2 \rangle$ computed for the fictitious noninteracting Kohn-Sham determinants is close to 2.0 for the triplets ($\langle \hat{S}^2 \rangle = 2.0053$) and to 1.0 for broken-symmetry states ($\langle \hat{S}^2 \rangle = 1.0053$)—note, however, that this is not the same as the expectation value of $\hat{S}^2$ in the true many-body wave function.

In the broken-symmetry state, one b_{1g} orbital with spin up is localized on one molecule; the other with spin down on the other molecule as shown in Fig. 9. Meanwhile, in the triplet state, two b_{1g} orbitals with spin up are localized on both molecules. This is consistent with the DFT calculation of isolated Cu(II)Pc molecule in which localized b_{1g} state carries the unpaired metal electron.

The predicted trend of the exchange couplings is consistent with perturbation-theory calculations shown in Fig. 8 and, in particular, shows a strong increase in the coupling as the molecules approach perfect π stacking ($\phi=90°$). For the β phase ($\phi=45°$), we have $J=E_{BS}-E_T=-1.1\times 10^{-6}$ hartree ≈ -0.3 K (see Fig. 10), in agreement with the experimental observation of a nearly paramagnetic state at accessible temperatures, and for α phase ($\phi=65°$), we have $J=E_{BS}-E_T=-5.5\times 10^{-6}$ hartree ≈ -1.7 K (see Fig. 10), which gives us a very good agreement with experimental observation $J\sim -1.5$ K.

The magnitude of the exchange couplings in Cu(II)Pc is very small, about 10^{-6} hartree, which is right at the edge of the accuracy of the DFT calculation, since there will be errors from the imperfect density functionals and from the finite basis sets as well as the numerical convergence errors discussed above. However, we can have some confidence in these results for three reasons. First, they agree remarkably well with the magnetization measurements made by the SQUID technique.[16] Second, many of the sources of DFT error could be expected to cancel when we compute the energy difference between systems that are so similar in every respect except for their spin orientation. Third, as discussed above, the results agree with the trends predicted by perturbation theory.

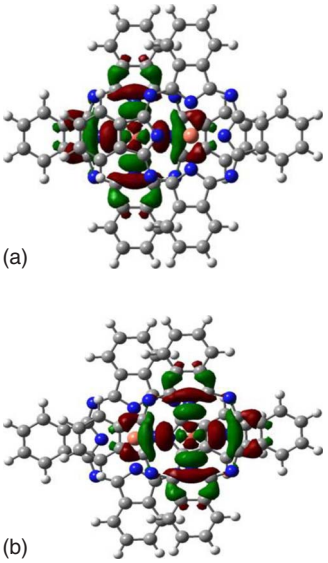

FIG. 9. (Color online) The broken-symmetry orbitals for unpaired electrons in each molecule with (a) spin up and (b) spin down from our DFT calculations for Cu(II)Pc dimer (stacking angle of 65°). Notice that b_{1g} states are localized on different molecules.

V. CONCLUSION AND DISCUSSION

From perturbative calculations of Cu(II)Pc and Mn(II)Pc, we find that the exchange interaction between two Cu(II)Pc molecules is dominated by indirect exchange. When the

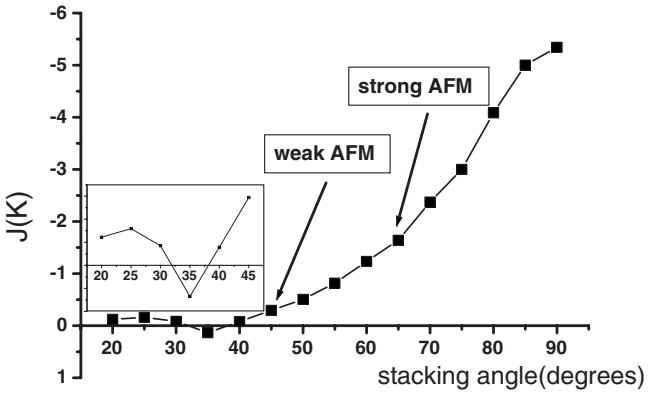

FIG. 10. The energy difference $J=E_{BS}-E_T$ as a function of stacking angle from 20° to 90°. Notice the qualitative consistency between this figure and Fig. 8.

stacking angle is 65°, the indirect exchange is predicted to be antiferromagnetic, while when the stacking angle is 45°, it is very weakly ferromagnetic. Both these results agree qualitatively with the experimental observations (see Sec. I).

In Mn(II)Pc, by contrast, both superexchange and indirect exchange contribute. The sign of the indirect exchange interaction in both cases is dependent on the sign of intermolecule electron transfer integrals and hence varies with stacking angle; however, the most important terms in the superexchange are always positive (antiferromagnetic).

The main discrepancy with the experiments is in the case of Mn(II)Pc, where our perturbative calculations do not give the very strong ferromagnetic interaction which was observed. This is probably because the true exchange interaction involves the competition between superexchange (always antiferromagnetic) and indirect exchange (predicted to be once again antiferromagnetic at 65°, weakly ferromagnetic at 45°), as well as possibly other routes. The different mechanisms involve different intramolecular couplings, and so this competition is very difficult to quantify on the basis of model calculations.

Despite the very different methodology, DFT calculations on Cu(II)Pc produce results that are remarkably consistent with the perturbation theory. When the angle becomes small, the oscillatory structure of exchange interactions calculated by both perturbation theory and DFT is a signature of the indirect exchange interaction, rather as conventional RKKY oscillations are in a normal metal.

ACKNOWLEDGMENTS

We wish to acknowledge the support of the UK Research Councils Basic Technology Programme under Grant No. GR/S23506. We thank Gabriel Aeppli, Sandrine Hertz, Chiranjib Mitra, Marshall Stoneham, Hai Wang, and Dan Wheatley for helpful discussions.

APPENDIX: INDIRECT EXCHANGE FOR Mn(II)Pc

First, we need to find the symmetry properties of the products of pairs of one-electron functions that appear in Eq. (13). Here, we consider the most complicated case, the product of two e_g states. Eventually, we will consider the scattering between filled and empty e_g levels in the molecule, through interaction with the e_g states of the Mn ion. To do this, we need the elements of the matrix X such that

$$X^{-1}[e_g \otimes e_g]X = a_{1g} \oplus b_{1g} \oplus a_{2g} \oplus b_{2g}, \tag{A1}$$

which are the Clebsch-Gordan coefficients for the product representation $e_g \otimes e_g$. We can label them as $X(\alpha, ij)$, where α refers to one of the irreducible representations appearing on the right of Eq. (A1), and i, j label the functions transforming as e_g. We find

$$X = \begin{array}{c} \\ xx \\ xy \\ yx \\ yy \end{array} \begin{array}{c} \begin{array}{cccc} a_{1g} & a_{2g} & b_{1g} & b_{2g} \end{array} \\ \begin{pmatrix} 1/\sqrt{2} & 0 & 1/\sqrt{2} & 0 \\ 0 & 1/\sqrt{2} & 0 & 1/\sqrt{2} \\ 0 & -1/\sqrt{2} & 0 & 1/\sqrt{2} \\ 1/\sqrt{2} & 0 & -1/\sqrt{2} & 0 \end{pmatrix} \end{array}. \tag{A2}$$

Because $\frac{1}{|\mathbf{r}-\mathbf{r}'|}$ belongs to the identity representation, we can then rewrite $\hat{v}$ as

$$\hat{v} = \sum_{\sigma,\sigma'} \sum_{\alpha} \int d\mathbf{r} d\mathbf{r}' \Psi^{(\alpha)*} \frac{1}{|\mathbf{r}-\mathbf{r}'|} \Psi^{(\alpha)} \times \sum_{ABDE} X(\alpha, AB) X^*(\alpha, DE) \hat{c}^{\dagger}_{A,\sigma} \hat{c}^{\dagger}_{B,\sigma'} \hat{c}_{D,\sigma'} \hat{c}_{E,\sigma},$$

$$= \frac{1}{2} \sum_{\alpha} \int d\mathbf{r} d\mathbf{r}' \Psi^{(\alpha)*} \frac{1}{|\mathbf{r}-\mathbf{r}'|} \Psi^{(\alpha)} \sum_{\sigma,\sigma'} \hat{O}^T M^{\alpha} \hat{P}, \tag{A3}$$

$$\hat{O} = \begin{pmatrix} \hat{c}^{\dagger}_{x,\sigma} \hat{c}^{\dagger}_{x,\sigma'} \\ \hat{c}^{\dagger}_{x,\sigma} \hat{c}^{\dagger}_{y,\sigma'} \\ \hat{c}^{\dagger}_{y,\sigma} \hat{c}^{\dagger}_{x,\sigma'} \\ \hat{c}^{\dagger}_{y,\sigma} \hat{c}^{\dagger}_{y,\sigma'} \end{pmatrix}, \tag{A4}$$

$$\hat{P} = \begin{pmatrix} \hat{c}_{x,\sigma'} \hat{c}_{x,\sigma} \\ \hat{c}_{x,\sigma'} \hat{c}_{y,\sigma} \\ \hat{c}_{y,\sigma'} \hat{c}_{x,\sigma} \\ \hat{c}_{y,\sigma'} \hat{c}_{y,\sigma} \end{pmatrix}, \tag{A5}$$

$$M^{a_{1g}} = \begin{pmatrix} 1 & 0 & 0 & 1 \\ 0 & 0 & 0 & 0 \\ 0 & 0 & 0 & 0 \\ 1 & 0 & 0 & 1 \end{pmatrix}, \tag{A6}$$

$$M^{a_{2g}} = \begin{pmatrix} 0 & 0 & 0 & 0 \\ 0 & 1 & -1 & 0 \\ 0 & -1 & 1 & 0 \\ 0 & 0 & 0 & 0 \end{pmatrix}, \tag{A7}$$

$$M^{b_{1g}} = \begin{pmatrix} 1 & 0 & 0 & -1 \\ 0 & 0 & 0 & 0 \\ 0 & 0 & 0 & 0 \\ -1 & 0 & 0 & 1 \end{pmatrix}, \tag{A8}$$

$$M^{B_{2g}} = \begin{pmatrix} 0 & 0 & 0 & 0 \\ 0 & 1 & 1 & 0 \\ 0 & 1 & 1 & 0 \\ 0 & 0 & 0 & 0 \end{pmatrix}, \tag{A9}$$

$$\Psi^{(A_{1g})} = \frac{1}{\sqrt{2}}(|xx\rangle + |yy\rangle), \tag{A10}$$

$$\Psi^{(A_{2g})} = \frac{1}{\sqrt{2}}(|xy\rangle - |yx\rangle), \tag{A11}$$

$$\Psi^{(B_{1g})} = \frac{1}{\sqrt{2}}(|xx\rangle - |yy\rangle), \tag{A12}$$

$$\Psi^{(B_{2g})} = \frac{1}{\sqrt{2}}(|xy\rangle + |yx\rangle). \tag{A13}$$

We use X, Y to label the ligand E_{gx}, E_{gy} states and x, y to label Mn e_{gx}, e_{gy} orbitals. Now, we introduce operators which create electron-hole excitations with different spin symmetries on the Pc:

$$a_i^{\dagger(0,0)} = a_i^{\dagger S} = \frac{1}{\sqrt{2}}(a_i^{\dagger\uparrow\downarrow} + a_i^{\dagger\downarrow\uparrow}), \tag{A14}$$

$$a_i^{\dagger(1,0)} = a_i^{\dagger T} = \frac{1}{\sqrt{2}}(a_i^{\dagger\uparrow\downarrow} - a_i^{\dagger\downarrow\uparrow}), \tag{A15}$$

$$a_i^{\dagger\uparrow\downarrow} = \hat{c}_{i_x\downarrow}^{\dagger}\hat{c}_{i_g\downarrow}, \quad a_i^{\dagger\downarrow\uparrow} = \hat{c}_{i_x\uparrow}^{\dagger}\hat{c}_{i_g\uparrow}, \tag{A16}$$

$$a_i^{\dagger(1,1)} = a_i^{\dagger\uparrow\uparrow} = \hat{c}_{i_x\uparrow}^{\dagger}\hat{c}_{i_g\downarrow}, \tag{A17}$$

$$a_i^{\dagger(1,-1)} = a_i^{\dagger\downarrow\downarrow} = \hat{c}_{i_x\downarrow}^{\dagger}\hat{c}_{i_g\downarrow}, \tag{A18}$$

where i runs over the two orientations of the ligand e_g states ($i=X,Y$) and the subscripts g,x of i label the filled ligand e_g states and LUMO ligand e_g states. The following operators characterize the spin degrees of freedom within the subspace where no charge transfer takes place:

$$S_j^z = \frac{1}{2}(n_{j\uparrow} - n_{j\downarrow}), \tag{A19}$$

$$S_j^{\dagger} = \hat{c}_{j\uparrow}^{\dagger}\hat{c}_{j\downarrow}, \tag{A20}$$

$$S_j^{-} = \hat{c}_{j\downarrow}^{\dagger}\hat{c}_{j\uparrow}, \tag{A21}$$

where j runs over all the e_g states of the Mn ion and the ligand: $j=X_x$, X_g, Y_x, Y_g, x, y. Using these operators, we can expand $\hat{v}$ as

$$\hat{v} = \hat{v}_1 + \hat{v}_2 + \hat{v}_3 + \text{spin-independent terms}, \tag{A22}$$

where

$$\begin{aligned}\hat{v}_1 = {} & (a_X^S + a_Y^S)[2\sqrt{2}(P_3 + P_4 - P_1/2 - P_2/2)] \\ & + 2\sqrt{2}a_X^T(P_1S_x^z + P_2S_y^z) + 2\sqrt{2}a_Y^T(P_2S_x^z + P_1S_y^z) \\ & + 2S_x^{\dagger}(P_1a_X^{\dagger\downarrow\downarrow} + P_2a_Y^{\dagger\downarrow\downarrow}) + 2S_y^{\dagger}(P_1a_Y^{\dagger\downarrow\downarrow} + P_2a_X^{\dagger\downarrow\downarrow}) \\ & - 2S_x^{-}(P_1a_X^{\dagger\uparrow\uparrow} + P_2a_Y^{\dagger\uparrow\uparrow}) - 2S_y^{-}(P_1a_Y^{\dagger\uparrow\uparrow} + P_2a_X^{\dagger\uparrow\uparrow}),\end{aligned} \tag{A23}$$

$$\begin{aligned}\hat{v}_2 = {} & 2(n_{x\uparrow}[-P_5n_{X_x\uparrow} - P_6n_{Y_x\uparrow}] + n_{x\downarrow}[-P_5n_{X_x\downarrow} - P_6n_{Y_x\downarrow}] \\ & + n_{y\uparrow}[-P_5n_{Y_x\uparrow} - P_6n_{X_x\uparrow}] + n_{y\downarrow}[-P_5n_{Y_x\downarrow} - P_6n_{X_x\downarrow}] \\ & + S_x^{\dagger}[-P_5S_{X_x}^{-} - P_6S_{Y_x}^{-}] + S_y^{\dagger}[-P_5S_{Y_x}^{-} - P_6S_{X_x}^{-}] \\ & + S_x^{-}[-P_5S_{X_x}^{\dagger} - P_6S_{Y_x}^{\dagger}] + S_y^{-}[-P_5S_{Y_x}^{\dagger} - P_6S_{X_x}^{\dagger}]),\end{aligned} \tag{A24}$$

$$\begin{aligned}\hat{v}_3 = {} & 2(n_{x\uparrow}[-P_5'n_{X_g\uparrow} - P_6'n_{Y_g\uparrow}] + n_{x\downarrow}[-P_5'n_{X_g\downarrow} - P_6'n_{Y_g\downarrow}] \\ & + n_{y\uparrow}[-P_5'n_{Y_g\uparrow} - P_6'n_{X_g\uparrow}] + n_{y\downarrow}[-P_5'n_{Y_g\downarrow} - P_6'n_{X_g\downarrow}] \\ & + S_x^{\dagger}[-P_5'S_{X_g}^{-} - P_6'S_{Y_g}^{-}] + S_y^{\dagger}[-P_5'S_{Y_g}^{-} - P_6'S_{X_g}^{-}] \\ & + S_x^{-}[-P_5'S_{X_g}^{\dagger} - P_6'S_{Y_g}^{\dagger}] + S_y^{-}[-P_5'S_{Y_g}^{\dagger} - P_6'S_{X_g}^{\dagger}]),\end{aligned} \tag{A25}$$

and

$$\begin{aligned}P_1 &= \{x,X_x|X_g,x\} + \{y,Y_x|Y_g,y\}, \\ P_2 &= \{x,Y_x|Y_g,x\} + \{y,X_x|X_g,y\}, \\ P_3 &= \{X_x,x|X_g,x\} + \{Y_x,y|Y_g,y\}, \\ P_4 &= \{X_x,y|X_g,y\} + \{Y_x,x|Y_g,x\}, \\ P_5 &= \{x,X_x|X_x,x\} + \{y,Y_x|Y_x,y\}, \\ P_6 &= \{x,Y_x|Y_x,x\} + \{y,X_x|X_x,y\}, \\ P_5' &= \{x,X_g|X_g,x\} + \{y,Y_g|Y_g,y\}, \\ P_6' &= \{x,Y_g|Y_g,x\} + \{y,X_g|X_g,y\}.\end{aligned} \tag{A26}$$

Here, we can see that $\hat{v}_1$ governs the creation of the electron-hole pair, while $\hat{v}_2$ and $\hat{v}_3$ represent the exchange interactions between spins on the Mn ion and on the ligand. Using this form of $\hat{v}$, we can build the Hamiltonian matrix for two sets of wave functions: those in which the total z component of spin on one molecule (Mn plus ligand) is, respectively, $+3/2$ and $+1/2$. We label the individual states as $|S_{\mathrm{Mn(II)}},S_{\mathrm{Pc}}\rangle$, where the first index is the spin configuration of Mn ion, and the second is the spin configuration of the ligand in the X or Y spatial component.

(1) The $+3/2$ states are $|(3/2),g\rangle$, $|(3/2),(S=0,M=0)\rangle$, $|(3/2),(S=1,M=0)\rangle$, and $|(1/2),(S=1,M=1)\rangle$, and the corresponding matrix is

$$\hat{v}_{3/2} = \begin{pmatrix} 0 & \beta & \frac{3}{2}\alpha & -\sqrt{\frac{3}{2}}\alpha \\ \beta & 0 & 0 & \gamma \\ \frac{3}{2}\alpha & 0 & 0 & \sqrt{6}\delta \\ -\sqrt{\frac{3}{2}}\alpha & \gamma & \sqrt{6}\delta & 0 \end{pmatrix}, \tag{A27}$$

where $\alpha=2\sqrt{2}/3(P_1+P_2)$, $\beta=2\sqrt{2}(P_3+P_4-1/2P_1-1/2P_2)$, $\gamma=\sqrt{6}/3(P_5'+P_6'-P_5-P_6)$, and $\delta=1/3(-P_5'-P_6'-P_5-P_6)$.

(2) The $+1/2$ states are $|(1/2),g\rangle$, $|(1/2),(S=0,M=0)\rangle$, $|(1/2),(S=1,M=0)\rangle$, $|(-1/2),(S=1,M=1)\rangle$, and $|(3/2),(S=1,M=-1)\rangle$, and the matrix of Coulomb interaction $\hat{v}_{1/2}$ is

$$\begin{pmatrix} 0 & \beta & 1/2\alpha & -\sqrt{2}\alpha & \sqrt{3/2}\alpha \\ \beta & 0 & 0 & 2/\sqrt{3}\gamma & -\gamma \\ 1/2\alpha & 0 & 0 & 2/\sqrt{2}\delta & \sqrt{6}\delta \\ -\sqrt{2}\alpha & 2/\sqrt{3}\gamma & 2\sqrt{2}\delta & 0 & 0 \\ \sqrt{3/2}\alpha & -\gamma & \sqrt{6}\delta & 0 & 0 \end{pmatrix}. \tag{A28}$$

To get the leading terms in the effective Hamiltonian (5), we need consider the situation where the total z-direction angular momentum on *both* molecules is $M_{total}=M_s^{\mathrm{Mn}_A}+M_s^{\mathrm{Mn}_B}+M_s^{\mathrm{Pc}}=2$. If we restrict ourselves to excitations in which there is only one electron-hole pair in total on the two Mn(II)Pc molecules, and suppose it resides in the X-symmetry orbitals (the Y-symmetry states are completely decoupled in the + model), we are left with a total of 18 states. These are made up as follows:

$$(M_s^{\mathrm{Mn}_A}=3/2, M_s^{\mathrm{Mn}_B}=1/2, M_s^{\mathrm{Pc}}=0) \rightarrow 5 \text{ states},$$

$$(M_s^{\mathrm{Mn}_A}=1/2, M_s^{\mathrm{Mn}_B}=3/2, M_s^{\mathrm{Pc}}=0) \rightarrow 5 \text{ states},$$

$$(M_s^{\mathrm{Mn}_A}=1/2, M_s^{\mathrm{Mn}_B}=1/2, M_s^{\mathrm{Pc}}=1) \rightarrow 2 \text{ states},$$

$$(M_s^{\mathrm{Mn}_A}=3/2, M_s^{\mathrm{Mn}_B}=-1/2, M_s^{\mathrm{Pc}}=0) \rightarrow 2 \text{ states},$$

$$(M_s^{\mathrm{Mn}_A}=-1/2, M_s^{\mathrm{Mn}_B}=3/2, M_s^{\mathrm{Pc}}=0) \rightarrow 2 \text{ states},$$

$$(M_s^{\mathrm{Mn}_A}=3/2, M_s^{\mathrm{Mn}_B}=3/2, M_s^{\mathrm{Pc}}=-1) \rightarrow 2 \text{ states}. \tag{A29}$$

The perturbation includes both the Coulomb interaction $\hat{v}$ discussed above and the hopping t which transfers an electron-hole pair from one Mn(II)Pc to another. We found the leading term of spin-$\frac{3}{2}$ couplings J_1 to be

$$J_1=\frac{3\alpha^2 t}{(U_g-U_x-E_x-2j_{\mathrm{eh}})^2}, \tag{A30}$$

where the definitions of U_g, U_x, E_x, j_{eh}, t_e, and t_g are the same as those in the Cu(II)Pc calculation.

Considering other situations such as the product of a_{1g} and e_g states gives qualitatively similar results that depend in the same way on the transfer integrals between molecules. Finally, we include excitations through both components (X and Y) of the ligand e_g states, so as in the Cu(II)Pc calculation, we should combine the electron-hole pair transfer integrals to form $t=t^x+t^y$.

*wei.wu@ucl.ac.uk
†Present address: UCL Department of Chemistry, 20 Gordon Street, London WC1H 0AJ, UK.
‡andrew.fisher@ucl.ac.uk

[1] M. Kinoshita, P. Turek, M. Tamura, K. Nozawa, D. Shiomi, Y. Nakazawa, M. Ishikawa, M. Takahashi, K. Awaga, T. Inabe, and Y. Maruyama, Chem. Lett. **1991**, 1225.
[2] J. Yoo, E. K. Brechin, A. Yamaguchi, M. Nakano, J. C. Huffman, A. L. Maniero, L.-C. Brunel, K. Awaga, H. Ishimoto, G. Christou, and D. N. Hendrickson, Inorg. Chem. **39**, 3615 (2000).
[3] A. W. Ghosh, P. S. Damle, S. Datta, and A. Nitzan, in MRS Symposia Proceedings No. 29 (Material Research Society Bulletin, Pittsburgh, 2004), p. 6.
[4] A. R. Rocha, V. M. García-Suárez, S. W. Bailey, C. J. Lambert, J. Ferrer, and S. Sanvito, Nat. Mater. **4**, 335 (2005).
[5] S. Pramanik, C.-G. Stefanita, S. Patibandla, S. Bandyopadhyay, K. Garre, N. Harth, and M. Cahay, Nat. Nanotechnol. **2**, 216 (2007).
[6] B. N. Engel, J. Akerman, B. Butcher, R. W. Dave, M. DeHerrera, M. Durlam, G. Grynkewich, J. Janesky, S. V. Pietambaram, N. D. Rizzo, J. M. Slaughter, K. Smith, J. J. Sun, and S. Tehrani, IEEE Trans. Magn. **41**, 132 (2005).
[7] E. G. Emberly and G. Kirczenow, Chem. Phys. **281**, 311 (2002).
[8] R. Pati, L. Senapati, P. M. Ajayan, and S. K. Nayak, Phys. Rev. B **68**, 100407(R) (2003).
[9] *The Porphyrins*, edited by David Dolphin (Academic, New York, 1979).
[10] C. G. Barraclough, R. L. Martin, and S. Mitra, J. Chem. Phys. **53**, 1638 (1970).
[11] H. Yamada, T. Shimada, and A. Koma, J. Chem. Phys. **108**, 10256 (1998).
[12] M. Evangelisti, J. Bartolomé, L. J. de Jongh, and G. Filoti, Phys. Rev. B **66**, 144410 (2002).
[13] S. Mitra, A. Gregson, W. Hatfield, and R. Weller, Inorg. Chem. **22**, 1729 (1983).
[14] M. Ashida, N. Uyeda, and E. Suito, Bull. Chem. Soc. Jpn. **39**, 2616 (1966).
[15] A. Hoshino, Y. Takenaka, and H. Miyaji, Acta Crystallogr., Sect. B: Struct. Sci. **B59**, 393 (2003).
[16] S. Heutz, C. Mitra, Wei Wu, A. J. Fisher, A. Kerridge, A. M. Stoneham, A. H. Harker, J. Gardener, H.-H. Tseng, T. S. Jones, C. Renner, and G. Aeppli, Adv. Mater. (Weinheim, Ger.) **19**, 3618 (2007).
[17] W. Heisenberg, Z. Phys. **49**, 619 (1928).
[18] J. C. Bonner and M. E. Fisher, Phys. Rev. **135**, A640 (1964).
[19] P. W. Anderson, Phys. Rev. **115**, 2 (1959).
[20] Wei Wu, P. T. Greenland, and A. J. Fisher, arXiv:0711.0084 (unpublished).
[21] M. A. Ruderman and C. Kittel, Phys. Rev. **96**, 99 (1954).
[22] N. F. Ramsey, Phys. Rev. **91**, 303 (1953).
[23] N. F. Ramsey, B. J. Malenka, and U. E. Kruse, Phys. Rev. **91**, 1162 (1953).
[24] N. Bloembergen and T. J. Rowland, Phys. Rev. **97**, 1679 (1955).
[25] T. Kasuya, Prog. Theor. Phys. **16**, 45 (1956).
[26] K. Yosida, Phys. Rev. **106**, 893 (1957).
[27] P. S. Bagus and B. I. Bennett, Int. J. Quantum Chem. **9**, 143 (1974).
[28] T. Ziegler, A. Rauk, and E. J. Baerends, Theor. Chim. Acta **43**, 261 (1977).
[29] L. Noodleman, J. Chem. Phys. **74**, 5737 (1980).
[30] K. Yamaguchi, T. Fueno, N. Ueyama, A. Nakamura, and M. Ozaki, Chem. Phys. Lett. **164**, 210 (1988).
[31] A. di Matteo and V. Barone, J. Phys. Chem. A **103**, 7676 (1999).
[32] R. L. Martin and F. Illas, Phys. Rev. Lett. **79**, 1539 (1997).
[33] F. Illas, I. de P. R. Moreira, C. de Graaf, and V. Barone, Theor. Chem. Acc. **104**, 265 (2000).
[34] J. A. Chan, B. Montanari, J. D. Gale, S. M. Bennington, J. W. Taylor, and N. M. Harrison, Phys. Rev. B **70**, 041403(R) (2004).
[35] A. D. Becke, Phys. Rev. A **38**, 3098 (1988).
[36] C. Lee, W. Yang, and R. G. Parr, Phys. Rev. B **37**, 785 (1988).

[37] A. D. Becke, J. Chem. Phys. **98**, 5648 (1993).
[38] M. J. Frisch *et al.*, GAUSSIAN 98, Gaussian, Inc., Pittsburgh, PA, 1998.
[39] R. Ditchfield, W. J. Hehre, and J. A. Pople, J. Chem. Phys. **54**, 724 (1970).
[40] M. Zerner and M. Gouterman, Theor. Chim. Acta **4**, 44 (1960).
[41] Mengsheng Liao, Inorg. Chem. **44**, 1941 (2005).
[42] B. E. Williamson, T. C. VanCott, M. E. Boyle, G. C. Misener, M. J. Stillman, and P. N. Schatz, J. Am. Chem. Soc. **114**, 2412 (1992).